Kinetic Modeling of the Thermal Destruction of Lewisite

Juan Carlos Lizardo Huerta, B. Sirjean, Laurent Verdier, R. Fournet, Pierre-Alexandre Glaude

Kinetic Modeling of the Thermal Destruction of Lewisite

J.-C. Lizardo-Huerta[1], B. Sirjean[1], L. Verdier[2], R. Fournet[1], P.-A. Glaude[1*]

[1] Laboratoire Réactions et Génie des Procédés, CNRS, Université de Lorraine

1 rue Grandville BP 20451 54001 Nancy Cedex, France

[2] DGA Maîtrise NRBC, Site du Bouchet, 5 rue Lavoisier, BP n°3, 91710 Vert le Petit, France

Corresponding author :

Pierre-Alexandre Glaude

Laboratoire Réactions et Génie des Procédés

1 rue Grandville BP 20451 54001 Nancy Cedex,

France

Email: pierre-alexandre.glaude@univ-lorraine.fr

Abstract

Organoarsenic compounds have been widely used as pesticides and chemical agents. Lewisite ($C_2H_2AsCl_3$), a blister agent, is a model of such compounds. A comprehensive detailed kinetic mechanism of combustion has been developed based on theoretical investigations. A benchmark allowed to select an appropriate methodology able to deal with such a heavy atom as As with precision and reasonable computational times. The density functional theory (DFT) method ωB97X-D was found to give the best results on target data. Core pseudo potentials were used for arsenic with the cc-pVTZ-PP basis set, whereas Def2-TZVP basis set was used for other atoms. The mechanism of the decomposition of lewisite includes all reactions involved in thermal decomposition and combustion mechanisms, including molecular and radical intermediates, and the decomposition reactions of small species containing arsenic. Simulation shows that lewisite decomposition starts around 700K and is very little sensitive to the presence of oxygen since the radical reactions involve mainly very reactive Cl-atoms as chain carriers. The main reaction paths have been derived. As experimentally observed, $AsCl_3$ is the main arsenic product produced almost in one-to-one yield, whereas acetylene is an important hydrocarbon product in pyrolysis. In combustion, several arsenic oxides, eventually chlorinated, are produced, which toxicity need to be assessed.

Keywords: lewisite, organoarsenic, decontamination, kinetic modelling, theoretical chemistry.

Introduction

Organic arsenical compounds have been widely used as pesticides or herbicides, e.g. the Blue Agent containing cacodylic acid or the Yellow Agent (HL), which is the eutectic mixture of Sulfur mustard (HD) and Lewisite (L) (Stone et al., 2016). This latter, the 2-chloroethenylarsonous dichloride ($C_2H_2AsCl_3$), has been manufactured as a chemical warfare agent used as vesicant and lung irritant (Baert and Danel, 2004; Gupta, 2015; Radke et al., 2014). Lewisite is also considered in the top of chemical agents for potential small-scale terrorist attacks because of its relatively simple synthesis, its severe health impact and the simplicity of dispersion (Shea and Gottron, 2004). The decontamination of material as well as the destruction of stockpiles and unexploded ammunitions still found on battlefields (Sanderson et al., 2014) by thermal treatments requires the development of highly safe processes based on well-defined kinetics (Bunnett et al., 1998). Lewisite is an oily colorless liquid with a geranium-like smell in its pure form but may have a color ranging from yellow to black depending on the amount of impurities. Lewisite has a high boiling point (about 190°C) and a melting point of -18°C which can vary depending on the purity (Radke et al., 2014) and is considered as persistent in contaminated soils (Sanderson et al., 2007). The blistering effect has been estimated to appear with doses as little as 2 ml on skin or vapor exposure in air from 0.06 to 0.33 mg/L, associated with a systemic toxicity, which can be lethal within several hours (National Research Council (US) Subcommittee on Chronic Reference Doses for Selected Chemical Warfare Agents, 1999). LD_{50} has been measured at a value of 50 mg/kg for the rat, while a NOAEL (no-observed-adverse-effect level) between 0.5 and 1.0 mg/kg/day was obtained from the rat for a 90-day oral subchronic toxicity (National Research Council (US) Subcommittee on Chronic Reference Doses for Selected Chemical Warfare Agents, 1999).

Lewisite, formed by the addition of trichloroarsine ($AsCl_3$) to acetylene (C_2H_2) catalyzed by a Lewis acid, is a mixture of the *cis* and *trans* isomers in a proportion of about 10% of the cis

isomer. It was found that the toxicity of the two isomers was identical and that it was therefore not necessary to separate them during the manufacture process. Smith *et al.* (Smith et al., 1995) identified in mixtures the "geminal" isomer dichloro (1-chlorovinyl) arsine; this third isomer was not observed previously because of its very low amount (<1%). Urban and von Tersch (Urban and von Tersch, 1999) performed a conformational analysis of lewisite isomers using ab-initio calculations and found that the trans isomer has an electronic energy lower than the cis isomer by about 0.6 kcal mol^{-1}, whereas the geminal isomer, is located at about 1 kcal mol^{-1} above the trans form. Early works on destruction of lewisite showed that the combustion products include acetylene, acetylene chloride and dichloride, arsenic trichloride $AsCl_3$, chlorine, methyl and vinyl chloride (Baronian, 1988). $AsCl_3$ was found to be approximatively produced in a one-to-one ratio with lewisite. This somewhat stable species has been found also in large amounts during the combustion of contaminated sawdust containing both arsenic and chlorine (Zhang et al., 2020). Detoxification of lewisite was theoretically studied by Sahu et al. (Sahu et al., 2013), who investigated the use of 2,3-dimercaptopropanol, an antidote called "British anti-lewisite". They found that the main detoxification reaction involves the breaking of a As—Cl bond to form a new As—S bond producing a non-toxic stable species (2-methyl-1,3,2-dithio arsolan-4-yl methanol). Zhang et al.(Zhang et al., 2014) investigated theoretically the reaction of OH radicals with lewisite. The reactions envisaged involved H and Cl-atom abstractions as well as an addition followed by an atom elimination. The most favorable reaction was found to be the addition-elimination yielding $AsCl_2$ radical and $CHClCH_2O$. The present work aims go beyond these studies by performing a comprehensive theoretical study of the thermal decomposition and of the combustion of lewisite to deduce its chemical pathways of decomposition as well as the most sensitive reactions during its gas-phase reaction.

Computational methods

Arsenic contains a large number of electrons (Z = 33) and the calculation methods used for the elements of the first rows for such thermochemical investigations in combustion (Khalfa et al., 2015; Lizardo-Huerta et al., 2018) are unsuitable. It is necessary to consider the relativistic effects due to the core electrons, which are generally described by pseudo-potentials in the orbital bases. A benchmark from methods proposed in the literature to treat heavy atoms such as arsenic was performed to determine the best compromise between computation time and precision. This benchmark focused on the calculation of known enthalpies of formation for molecules containing As. Enthalpies of formation were calculated at 298 K for a set of molecules (As_2, AsH, AsH_2, AsH_3, AsF, AsF_2 and AsF_3) and compared to values from Feller et al.(Feller et al., 2011) taken as references. These authors performed calculations at the CCSD(T)/cc-pV6Z level, which is a very powerful method for taking into account the electron correlation, with a very large basis set and some adjustments to take into account an infinite basic extrapolation as well as the relativistic effects. However, such a calculation cost is far too high for lewisite, which also contains carbon and chlorine atoms.

First, we checked the performance of four density functionals (B3LYP, M06-2X, mPWLYP and ωB97X-D), associated with extended basis sets 6-311++G(3df,3pd) and Def2-TZVP. Enthalpies of formation were derived by atomization and compared to the dataset calculated by Feller et al. Calculations were performed with Gaussian09 (Frisch et al., 2009). Table 1 indicates deviations and the mean quadratic deviations from the reference data for the seven molecules for each level of theory. The ωB97X-D method with the Def2-TZVP basis set appears to produce the lowest deviation from reference data. Furthermore, the Def2-TZVP basis set makes it possible to reach the infinite basis energy(Weigend and Ahlrichs, 2005) for an affordable calculation cost. The Def2-TZVP basis set is recommended for DFT calculations of light elements and transition elements up to krypton. However, a large number of heavy atoms leads to a considerable increase in computation time. A solution is to use the Def2-TZVP basis set for atoms other than arsenic and a specific base for As with a pseudo-

potential for describing the frozen core electrons and which accounts also for relativistic effects. To select the appropriate electron core potential (ECP), tests were performed at the ωB97X-D level of theory considering different basis sets for arsenic, in which the number of frozen core electrons varies.

Table 1: Deviation and mean-square deviation of enthalpies of formation at 298K of the dataset calculated with different functionals and basis sets compared to reference data from (Feller et al., 2011) (kcal mol^{-1}).

	AsH	AsH_2	AsH_3	AsF	AsF_2	AsF_3	As_2	*MSD*
$\Delta H_{f.298K}$(Feller et al., 2011)	56.8±0.1	39.5±0.1	16.9±0.2	–9.4±0.2	–96.8±0.3	–195.0±0.6	45.6±0.3	
method	Basis set: 6-311++G(3df.3pd)							
B3LYP	-0.7	-2.1	-1.4	0.6	1.3	5.9	5.4	*3.2*
M06-2X	2.8	6.2	11.1	5.2	6.5	8.0	25.0	*11.6*
mPWLYP	-1.4	-3.2	-2.4	-7.4	-13.2	-13.5	-4.6	*8.1*
*ω*B97X-D	-0.7	-2.9	-3.0	-1.1	-2.4	-0.3	1.3	*2.0*
	Basis set: Def2-TZVP							
B3LYP	-0.5	-1.9	-1.1	1.1	1.9	6.4	5.7	*3.5*
M06-2X	2.3	5.2	9.8	3.5	3.8	4.6	20.3	*9.2*
mPWLYP	-1.3	-3.1	-2.4	-7.0	-12.8	-13.2	-4.4	*7.8*
*ω*B97X-D	-0.6	-2.6	-2.6	-0.2	-0.8	2.0	0.9	*1.7*

Six basis sets have been tested and the corresponding ECPs for arsenic have been retrieved from the EMSL Basis Set Exchange (Schuchardt et al., 2007). The number of core frozen electrons for arsenic are 10, 18 and 28 electrons depending on the basis set. The results presented in Table 2 give the differences between the present calculations and those obtained in (Feller et al., 2011). Remember that for all the elements except As, the Def2-TZVP basis set is used. It can be seen that freezing 28 electrons produces large deviations compared to the values of Feller *et al.* (SDD and LANL2DZ). The CRENBL base, in which 18 electrons are frozen, gives good results for the lightest species (AsH_n), but becomes much less efficient for the heavier species (As_2 and AsF_n). Methods freezing 10 electrons (cc-pVTZ-PP) lead to a good agreement with the literature, for all the species considered. Eventually, the ωB97X-D/cc-pVTZ-PP level of theory was adopted for arsenic and ωB97X-D/ Def2-TZVP level of theory for other atoms because of the favorable balance between precision and computation

time. This is an important criterion given the number of heavy atoms in lewisite and calculations needed to describe the thermochemistry of this compound.

Table 2: Deviation of enthalpies of formation at 298K calculated at the *ω*B97X-D level of theory using ECPs compared to data from (Feller et al., 2011) (kcal mol^{-1}).

Level of theory *ω*B97X-D/	Number of frozen electrons in As	AsH	AsH_2	AsH_3	AsF	AsF_2	AsF_3	As_2	*MSD*
cc-pVTZ-PP	10	-0.2	-1.7	-1.0	-0.2	-0.6	2.6	1.8	*1.4*
cc-pVQZ-PP	10	-0.4	-2.0	-1.4	-1.3	-2.9	-0.8	1.4	*1.6*
cc-pV5Z-PP	10	-0.4	-2.0	-1.5	-1.5	-3.2	-1.4	1.5	*1.8*
CRENBL	18	0.8	-0.5	-0.6	2.9	5.2	11.3	27.4	*11.4*
SDD	28	5.2	6.7	8.5	12.0	21.5	32.9	31.9	*20.2*
LANL2DZ	28	6.8	10.2	13.0	21.5	42.7	68.9	36.2	*35.2*

Pronicheva et al. (Pronicheva et al., 1992) have experimentally determined the structural parameters of the *trans* isomer of lewisite via gas-phase electron diffraction. These values are presented in Table 3, as well as that calculated by Saeidian and Sahandi (Saeidian and Sahandi, 2015), at the B3LYP/6-311++G(3df, 3pd) level of theory, and our calculations at the ωB97X-D/Def2-TZVP level of theory, which agree with the experimental results.

Table 3: Experimental and calculated structural parameters of *trans*-lewisite and error with respect to experimental data for the *ω*B97X-D/Def2-TZVP level of theory.

Geometrical parameters	Experimental (Pronicheva et al., 1992)	B3LYP/6-311++G(3df,3pd) (Saeidian and Sahandi, 2015)	ωB97X-D/ Def2-TZVP	Error (%)
Bond lengths (Å)				
As—C	1.891	1.943	1.933	2.2
As—Cl	2.197	2.209	2.184	-0.6
C=C	1.374	1.325	1.322	-3.8
C—H	0.961	1.082	1.083	12.7
C—Cl	1.729	1.730	1.723	-0.3
Bond angles (°)				
CAsCl	101.1	96.7	96.7	-4.4
ClAsC	99.1	99.2	99.3	0.2
CCAs	121	117.7	117.3	-3.0
CCH	127.8	122.7	122.7	-4.0
ClCC	121.3	123.8	123.7	2.0
Dihedral ClAsCC	162.1	129.9	129.9	-19.9

Most sensitive reactions were studied in this work, as well as the thermochemical data of reactants and intermediates. Electronic structure of the reactants, products and transition states (TS) have been computed with the method described above. An analysis of vibrational frequencies was systematically performed to confirm the nature of the TS and Intrinsic Reaction Coordinate (IRC) approach has been used, when necessary, to ensure the correct connection between a given transition state structure and the reactant and product. In addition, the low frequency vibration modes, corresponding to internal rotations, were treated as hindered rotors instead of harmonic oscillators, using THERMROT software (Lizardo-Huerta et al., 2016). This in-house code allows a one-dimensional hindered rotor (1D-HR) treatment of internal rotations and avoids the coupling of torsional modes encountered in the frequency analysis made by Gassian09. Note that quantum tunneling was considered using the Eckart approach for reactions involving H-atom transfers. High pressure limit rate constants were eventually calculated as a function of temperature using the Transition State Theory and were fitted using the three-parameter modified Arrhenius equation ($A \times T^n \times \exp(-E_a/RT)$) over the temperature range 300-2000 K.

Kinetic modelling

The model is composed of 3 sub-mechanisms: (i) a combustion mechanism from the laboratory, for C_0-C_2 hydrocarbons and benzene (Nowakowska et al., 2014); (ii) a mechanism proposed by Leylegian et al. to describe the reactions of chlorinated species (Leylegian et al., 1998), with updates for HCl combustion (Pelucchi et al., 2015); (iii) a mechanism specific to the combustion of lewisite developed in this work. In this latter, molecular eliminations, unimolecular and bimolecular initiations, H and Cl-atom abstractions, additions on the double bond, decomposition of the radicals formed, reactions between chlorine and arsenic, and decomposition reactions of light species containing arsenic were included. The rate constants were either taken directly from the literature or theoretically calculated at the ωB97XD/Def2-

TZVP/cc-pVTZ-PP level of theory. The detailed kinetic mechanism has been developed for *trans* and *cis* isomers of lewisite. The bond dissociation energies (BDE) presented in Figure 1 show that the weakest bond is the C—As bond, followed by the As—Cl bond. On the other hand, the C—Cl and C—H bond dissociation energies are the highest because the Cl and H atoms are linked to vinyl carbon atoms.

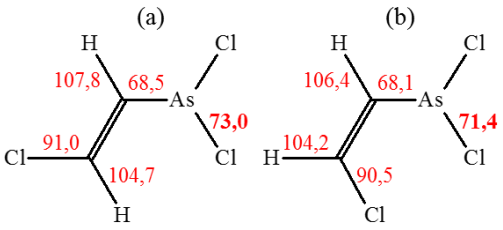

Figure 1. Chemical structure of (a) *trans* and (b) *cis* lewisite and bond dissociation energies computed at the ωB97XD/Def2-TZVP/cc-pVTZ-P level of theory (kcal mol^{-1}).

Pericyclic reactions. Four-centered eliminations are possible in *cis* and *trans* lewisite by transferring a H and a Cl-atom on the As atom. Both reactions were investigated theoretically. The second reaction, which transfer a Cl-atom, was found to involve a much lower energy barrier, as shown in Figure 2.

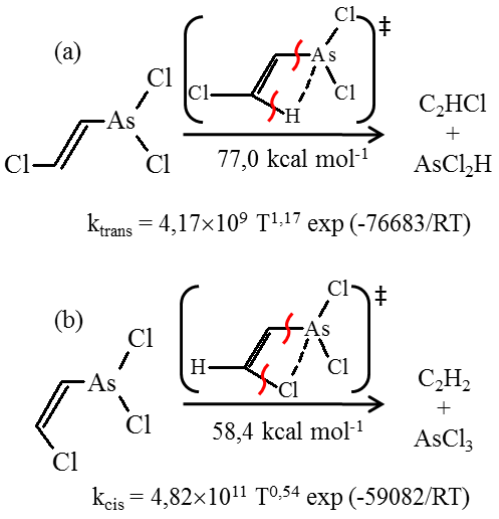

Figure 2. Pericyclic decomposition of (a) *trans* and (b) *cis* lewisite with energy barriers at 298 K and theoretically calculated rate constants in cm^3, mol, s, cal.

Radical Initiations. The unimolecular initiations involve the break of the C—As, As—Cl, C—Cl and C—H bonds. The kinetic coefficients were estimated from the correlations used in EXGAS (Buda et al., 2005), considering the inverse reactions of combination of the radicals. Bimolecular initiations with O_2 were included in the case of the H-atom abstractions yielding HO_2.

Atom Abstractions. Abstractions of the arsenic-bound chlorine atoms have been considered because of the low BDE compare to carbon-bound chlorine and hydrogen atoms. Reactions with the most reactive atoms and radicals (H, Cl, O, OH, $AsCl_2$ and CH_3) have been included. The rate constants were theoretically determined in the case of Cl-atom abstractions by OH and $AsCl_2$ radicals, while for H, Cl, O and CH_3, rate constants were estimated by analogy with CCl_4 (Louis et al., 2004; Huybrechts et al., 1996). The C—Cl BDE in CCl_4 (71.9 kcal mol^{-1}) is of the same order of magnitude as As—Cl BDE in lewisite (73 kcal mol^{-1}). H and Cl-atom abstractions from the carbon atoms were included in a first guess, but were found negligible and were removed. Rate constant are displayed in Table 4.

Table 4: Rate constants of atom abstraction from lewisite, in the form $k = A\ T^n \exp(-E / RT)$, in cm^3, mol, s, cal.

Reaction	A	n	E	Ref.
1. Lewisite+H = ClC_2H_2AsCl+HCl	1.57×10^9	1.63	4340	(Louis et al., 2004)
2. Lewisite+Cl = ClC_2H_2AsCl +Cl_2	5.75×10^{13}	0	15500	(Huybrechts et al., 1996)
3. Lewisite+O = ClC_2H_2AsCl +ClO	3.00×10^{11}	0	4370	(Herron, 1988)
4. Lewisite+OH = ClC_2H_2AsCl +HOCl	1.30×10^6	2.224	18150	This work
5. Lewisite+$AsCl_2$ = ClC_2H_2AsCl +$AsCl_3$	6.82×10^2	3.021	12630	This work
6. Lewisite+CH_3 = ClC_2H_2AsCl +CH_3Cl	1.26×10^{12}	0	9900	(Matheson et al., 1982)

Additions on double bond. Additions of OH, O and Cl on the C=C double bond were considered. Rate constants are presented in Table 5. For the reactions with O and Cl, the rate constants were estimated from the inverse reaction of β-scission by analogy with similar reactions in the literature. The rate constant of the addition of OH on the terminal vinyl carbon was calculated to be $2.55\times10^{12}\ T^{0.307}\exp(-35880/RT)$ $cm^3\ mol^{-1}\ s^{-1}$. The subsequent reactions of the adduct were investigated theoretically in a comprehensive way. The main channel was found to be an intramolecular isomerization of the adduct followed by a decomposition to CH_2=$AsCl_2$ and CHClO. The addition of O and OH on the carbon atom bounded to As leads to the breaking of the weak C—As bond and the formation of $AsCl_2$, while the other fragment undergoes a rearrangement to 2-chloro acetaldehyde, as presented in Figure 3. Rate constants were estimated by analogy with similar reactions, unless the addition of OH on the terminal carbon atom involving a higher barrier, which has been calculated theoretically. Rate constants for *cis*-lewisite were estimated as that of the *trans* isomer.

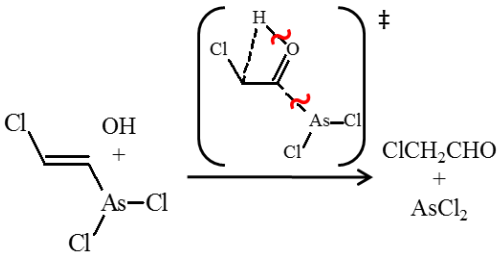

Figure 3. Addition of OH on C-atom bounded to As in lewisite

Table 5: Rate constants of addition to lewisite, in the form $k = A\ T^n \exp(-E / RT)$, in cm^3, mol, s, cal.

Reaction	A	n	E	Ref.
1. Lewisite+OH = CH_2ClCHO+$AsCl_2$	1.37×10^{12}	0	-1040	(Buda et al., 2005)
2. Lewisite+OH = $ClCH(OH)CHAsCl_2$	2.55×10^{12}	0.307	35880	This work
3. Lewisite+O = CH_2AsCl_2 +CClO	1.32×10^{8}	1.55	430	(Tsang and Hampson, 1986)

4. Lewisite+O = CHClCHO +$AsCl_2$	3.27×10^{12}	0	670	(Zhang et al., 2007)
5. Lewisite+Cl = $CCl_2HCHAsCl_2$	3.16×10^{12}	0	1000	(Ashmore et al., 1982)
6. Lewisite+Cl = ClCHCH(Cl)$AsCl_2$	1.82×10^{15}	0	3990	(Ayscough et al., 1961)

Additions of arsenic radicals on O_2. The main arsenic radicals, i.e. ClCHCHAsCl and $AsCl_2$, react slowly by decomposition, which permits to react with O_2 to form peroxy radicals ClCHCHAsClOO and $AsCl_2OO$ (reactions 1 and 4 in Table 6). These radicals can isomerize by an internal Cl-atom transfer from arsenic toward the O-atom (reactions 2 and 5) and therefore decompose (reactions 3 and 6). ClCHCHAsClOO radical can either react by an intramolecular H-atom transfer yielding $ClC_2HAsClOOH$ (reaction 7), followed by a radical β-scission (reaction 8). AsClOOH decomposes very easily into AsOCl and OH radical (reaction 9). Rate constants were determined theoretically except the barrierless additions 1 and 4, which were estimated by analogy with the reaction of CCl_3 (Russell et al., 1990).

Table 6: Reactions of arsenic radicals with O_2, rate constants in the form $k=AT^n\exp(-E/RT)$, in cm^3, mol, s, cal.

Reaction	A	n	E	Ref.
1. $AsCl_2+O_2 = AsCl_2OO$	7.00×10^{20}	-3.6	0	(Russell et al., 1990)
2. $AsCl_2OO = AsClOOCl$	1.13×10^{11}	0.437	58970	This work
3. $AsClOOCl = AsOCl+ClO$	7.03×10^{11}	0.517	3480	This work
4. $ClCHCHAsCl +O_2 = ClCHCHAsClOO$	7.00×10^{20}	-3.6	0	(Russell et al., 1990)
5. $ClCHCHAsClOO = ClCHCHAsOOCl$	1.13×10^{11}	0.437	58970	This work
6. $ClCHCHAsOOCl = ClC_2H_2AsO +ClO$	7.03×10^{11}	0.517	3480	This work
7. $ClCHCHAsClOO = ClC_2HAsClOOH$	5.25×10^{01}	2.758	24920	This work
8. $ClC_2HAsClOOH = C_2HCl+AsClOOH$	1.40×10^{15}	-0.228	14170	This work
9. $AsClOOH = AsOCl+OH$	4.89×10^{12}	0.349	8960	This work

Decomposition of radicals. The different radicals formed in the primary mechanism of the combustion of lewisite are decomposed by isomerization, cis/trans interconversions and β-

scissions. ClCHCHAsCl radical, produced by unimolecular initiation of lewisite, can be converted to cis-ClCHCHAsCl (reaction 1 in Table 7), followed by an internal transfer of Cl (reaction 2). The product then decomposes into acetylene and $AsCl_2$ by a β-scission (reaction 3). ClCHCHAsCl radical can also we by internal H-atom transfer (reaction 4) followed by a β-scission of the product, into C_2HCl and AsClH (reaction 5). $ClCCHAsCl_2$ decomposes by β-scission into C_2HCl and $AsCl_2$ (reaction 6). ClCHCClHAsCl2 produsedby the addition of a Cl-atom on the double bond decomposes to dichloroethylene and $AsCl_2$ (reaction 7). Theoretically computed rate constants are presented in Table 7.

Terminations. Combinations of the radicals $AsCl_2$, AsClH and CHCHCl with each other or with H, OH and Cl are considered. The corresponding kinetic parameters are those used in the hydrocarbon studies and involve a zero activation barrier(Buda et al., 2005).

Table 7: Rate constants of decomposition of the radicals derived from lewisite, in the form $k=AT^n\exp(-E/RT)$, in cm^3, mol, s, cal.

Reaction	A	n	E	Ref.
1. ClCHCHAsCl = cis-ClCHCHAsCl	2.08×10^{12}	0.354	29130	This work
2. cis-ClCHCHAsCl = $C_2H_2AsCl_2$	2.45×10^{13}	0.002	51090	This work
3. $C_2H_2AsCl_2 = C_2H_2 + AsCl_2$	4.36×10^{13}	0.119	8270	This work
4. ClCHCHAsCl = ClCCHAsClH	2.79×10^{7}	1,695	48470	This work
5. ClCCHAsClH = C_2HCl + AsClH	1.17×10^{14}	0.002	15110	This work
6. $ClCCHAsCl_2 = C_2HCl + AsCl_2$	1.40×10^{15}	-0.228	14170	This work
7. $ClCHCClHAsCl_2$ = CHClCHCl+$AsCl_2$	3.63×10^{12}	0.175	6280	This work

The thermochemical properties were taken from the literature in the case of species involved in the hydrocarbon and chlorine sub-mechanisms, and theoretically calculated for lewisite and related arsenic containing products. The theoretically calculated thermochemical data of the main arsenical species are presented in Table 8.

Table 8: Thermochemical properties of lewiste and related species determined at the ωB97XD / Def2-TZVP / cc-pVTZ-PP level of theory.

	$\Delta_f H^\circ_{298}$	S°_{298}	$C_p^\circ(T)$ **(**$calmol^{-1}K^{-1}$)

	(kcal mol^{-1})	($calmol^{-1}K^{-1}$)	300 K	500 K	800 K	1000 K	1500 K	2000 K
trans-lewisite	-23.96	97.23	27.47	31.82	35.60	37.12	39.43	40.69
cis-lewisite	-23.49	93.94	26.28	32.13	36.53	38.01	39.85	40.71
trans-ClCH=CH-AsCl	18.15	86.66	22.88	25.42	27.35	28.81	30.77	32.03
cis-ClCH=CH-AsCl	18.08	86.25	22.01	25.26	27.74	29.60	31.95	33.12
$ClC=CH-AsCl_2$	31.51	99.85	26.02	28.16	29.73	30.87	32.37	33.34
trans-ClCH=CH-AsO	12.90	82.57	20.93	25.93	30.36	32.00	34.12	35.22
cis-ClCH=CH-AsO	14.50	81.95	21.06	26.79	30.98	32.26	34.04	35.04
$HOC(Cl)=CH-AsCl_2$	-85.20	105.67	31.02	36.66	40.52	41.98	44.42	45.64
AsCl	48.53	58.52	8.33	8.69	8.84	8.87	8.91	8.93
$AsCl_2$	-22.44	71.75	12.64	13.48	13.71	13.74	13.85	13.88
$AsCl_3$	-65.29	80.28	17.88	19.22	19.56	19.60	19.78	19.82
AsClH	9.66	64.38	10.06	11.23	12.18	12.59	13.20	13.49
$AsClH_2$	-7.18	64.19	11.27	12.66	13.79	14.71	16.08	17.02
$AsCl_2H$	-34.57	72.50	14.15	16.35	17.77	18.27	19.04	19.40
AsOCl	-36.96	66.71	11.53	12.63	13.30	13.48	13.71	13.80
HOAsO	-66.31	65.85	12.80	14.56	15.91	16.90	18.10	18.60
$AsCl_2OH$	-94.20	79.37	19.91	22.67	23.44	23.44	23.82	24.08

Simulations

The model of lewisite combustion is composed of 320 species and 1749 reactions. The reactivity of this toxic under pyrolysis or combustion conditions was simulated in an isothermal closed reactor, with the Chemkin II software (Kee et al., 1993). The conditions were temperatures between 600 and 1100 K, a pressure of 1 bar and the residence time between 0 and 2 s. In pyrolysis, the initial concentration of lewisite (blend 90% *trans* + 10% *cis* lewisite) is 5% in N_2. In combustion, the same concentration was considered in air, which corresponds to an equivalence ratio of 0.67. The stoichiometry in combustion was set according to the following reaction:

$$10 \text{ lewisite} + 25\ O_2 \rightarrow 20\ CO_2 + 2\ H_2O + 4\ AsCl_3 + 2\ AsOCl + 2\ As_2O_3 + 16\ HCl.$$

Arsenic final products were set according to thermochemical equilibrium and to insure chlorine and hydrogen atom balance.

Figure 4 shows the conversion of lewisite in pyrolysis and combustion as a function of temperature, for a residence time of 2 s. Lewisite shows identical reactivity both in pyrolysis and combustion, with an onset of decomposition at 700 K and a total conversion around

820 K. As discussed below, the absence of difference is due to the importance of unimolecular decomposition and of the role of Cl-atom as chain carrier, whereas oxygen influence mostly the oxidation of light carbon containing products at temperatures, at which lewisite is already decomposed.

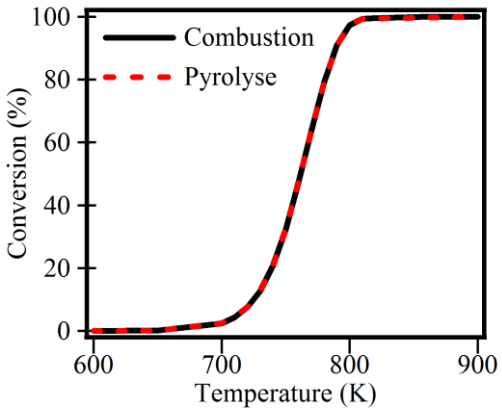

Figure 4. Conversion of 5 % lewisite in nitrogen and in air in a close vessel. P = 1 bar, τ = 2s.

The detailed speciation in pyrolysis and in combustion as a function of temperature are presented in Figures 5 and 6, respectively. In pyrolysis, lewisite starts to decompose around 700 K. The major product over all the temperature range is $AsCl_3$, which is obtained in about one-to-one ratio observed experimentally in the literature (Baronian, 1988). At high temperature, the amount of the little reactive $AsCl_2$ radical becomes noticeable. Acetylene is an important product that reaches a maximum around 950 K, and reacts mainly to form vinylacetylene C_4H_4 when temperature increases. Other important intermediates are chloroacetylene C_2HCl, dichloroethylene CHClCHCl and HCl, in accordance with experimental observations(Baronian, 1988). In combustion, the main decomposition product is again $AsCl_3$, but the typical products of the combustion of hydrocarbons are produced in large amounts (CO, CO_2 and H_2O). Other important arsenic containing products are AsOCl, HOAsO, while a lot of hydrochloric acid is present at high temperature. Intermediates are C_2HCl, C_2H_2, CHClCHCl as in pyrolysis, and $AsCl_2OH$. Note the two maxima of

chloroacetylene C2HCl profile: a first peak around 850 K results from lewisite decomposition through the formation of the chlorovinyl radical CHCHCl, a second around 950 K is due to the decomposition of 1,2-dichloroethylene CHClCHCl, which is one the main primary products of lewisite and is known to produces mono chloroacetylene (Goodall and Howlett, 1956).

Most of these products induce environmental and toxicological concerns. Trichloroarsine $AsCl_3$ is at ambient conditions a colorless liquid, with a vapor pressure around 1500 Pa at 25°C (Stull, 1947). The oral rat LD50 is 138 mg/kg and the fatal human dose lies between 70 and 180 mg depending on weight (Cheremisinoff, 1999). $AsCl_3$ produces chromosomal aberrations and reproductive effects on mice (Nagymajtényi et al., 1985). In presence of organic matter, it can lead to organic arsenicals such as methyldichloroarsine, which are vesicant and systemic poisons (Gupta, 2015). Inorganic arsenic oxides are often considered to have a toxicity close to arsenic. Arsenic trioxide As_2O_3 would be fatal to human at a dose of 120 mg (Baronian, 1988). Toxicology of arsenic oxychloride AsOCl and of chloroacetylene C_2HCl have not been studied because of their high reactivity but both are known as toxic. The latter is highly toxic and spontaneously flammable in contact with air (Pohanish, 2008).

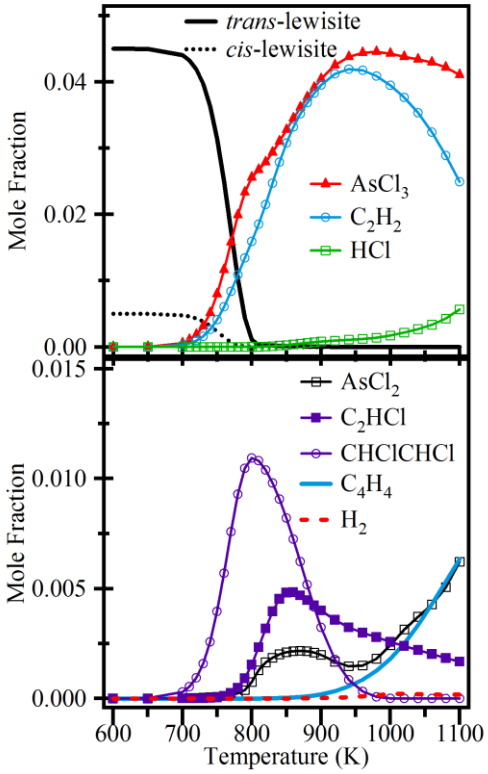

Figure 5: Pyrolysis of 5% lewisite in N_2 in a close vessel as a function of temperature. P = 1 bar, τ = 2 s.

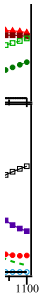

Figure 6: Combustion of lewisite in air (Φ=0.67) in a close vessel as a function of temperature. P = 1 bar, τ = 2 s.

Reaction pathways are investigated in pyrolysis and combustion. A flow analysis is presented in Figure 7, in conditions of Figures 5 and 6, at a temperature of 973 K representative of incineration conditions. The residence time of 0.4 ms corresponds to a conversion around 30%. It appears that *cis* and *trans*-lewisite decompose mainly through three pathways: by unimolecular initiation by breaking the C—As bond, by a Cl-atom abstraction from the arsenic atom by the radical $AsCl_2$ and by addition of the Cl-atom on the double bond. Unimolecular initiation leads to the formation of $AsCl_2$ and chlorovinyl radicals. $AsCl_2$ radicals participates in the conversion of lewisite through the Cl-atom abstractions. The chlorovinyl radical is decomposed by β-scission into C_2H_2 (100% of the flux in pyrolysis and 85% in combustion). In oxidation, a fraction of chlorovinyl (15%) leads to the formation of oxygenated and chlorinated products.

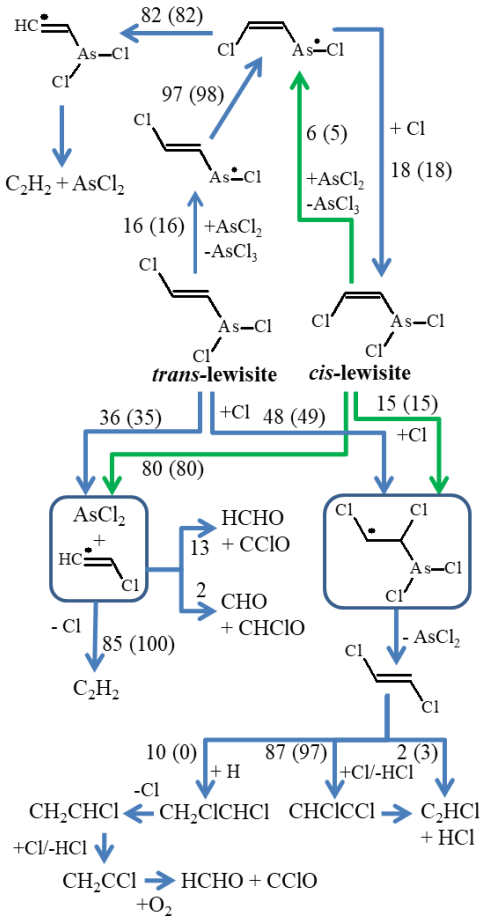

Figure 7: Flow analysis of decomposition of lewisite under pyrolysis and combustion conditions. T=973 K, P = 1 bar, $\tau = 4\ 10^{-4}$ s. Numbers correspond to the percentage in the flux of consumption of a species. Numbers in parenthesis correspond to pyrolysis.

The decomposition by Cl-atom abstraction leads to the formation of the ClCHCHAsCl radical. This radical is stabilized by resonance, which favors a possible *cis*/*trans* interconversion. The *cis*-ClC_2H_2AsCl radical isomerizes mainly by an internal Cl-atom transfer to $C_2H_2AsCl_2$ radical, which formation is not possible from the *trans*-ClC_2H_2AsCl. $C_2H_2AsCl_2$ decomposes thereafter by β-scission into C_2H_2 and $AsCl_2$. Note that part of the *cis*-ClC_2H_2AsCl radical yields back *cis*-lewisite by combination with a chlorine atom. Regarding products of the addition of chlorine to lewisite, $CHClCHClAsCl_2$ radicals decomposes by β-scission into $AsCl_2$ and 1,2-dichlorethylene (CHCl=CHCl). The latter decomposes mainly in HCl and C_2HCl by abstractions of a H-atom by a Cl-atom, followed by

the β-scission of the radical produced. In combustion, CHCl=CHCl decomposes also by addition of a H atom on the double bond, followed by β-scission, atom abstraction and oxidation reactions to finally yield formaldehyde and CClO. It can be seen that the main reactions pathways of decomposition of lewisite are the unimolecular decomposition and radical reactions involving Cl-atoms and $AsCl_2$ radicals as chain carriers in both pyrolysis and combustion. This explains the almost identical reactivity of lewisite whatever the oxygen content. This latter reacts only with hydrocarbon products and leads to the formation of combustion products. Note however that some chlorinated arsenic oxides are produced in combustion in addition to $AsCl_3$ as arsenic containing products, which toxicity needs to be assessed. The most sensitive reaction in all conditions is the initial C—As bond breaking, and in a much smaller extend, the Cl-atom abstraction by $AsCl_2$, and the decomposition of C_2H_2Cl into acetylene and Cl, which regenerate the chain carrier. The most inhibiting reactions are the combinations of Cl-atom and ClC_2H_2AsCl yielding back *trans* and *cis*-lewisite.

Another flow analysis was performed in combustion in air at 773K for an equivalent conversion of 30%, corresponding to a residence time of 0.7s. The global reaction scheme remains unchanged (Figure 8), but propagation chain length increases and Cl-atom abstractions by $AsCl_2$ accounts for 56% of lewisite consumption, while unimolecular decomposition ratio decreases to 20%. Another notable difference is the addition of the produced radical ClCHCHAsCl on O_2 that accounts for 8% of its consumption. After an internal Cl-atom shift, it decomposes into ClO and ClCHCHAs=O. This new channel has no kinetic influence on the global reactivity but is a source of arsenic oxide that can be important at low temperature. Note that the most sensitive reaction remains as at high temperature the Cl-atom abstraction from lewisite and the unimolecular Ac—Cl bond breaking.

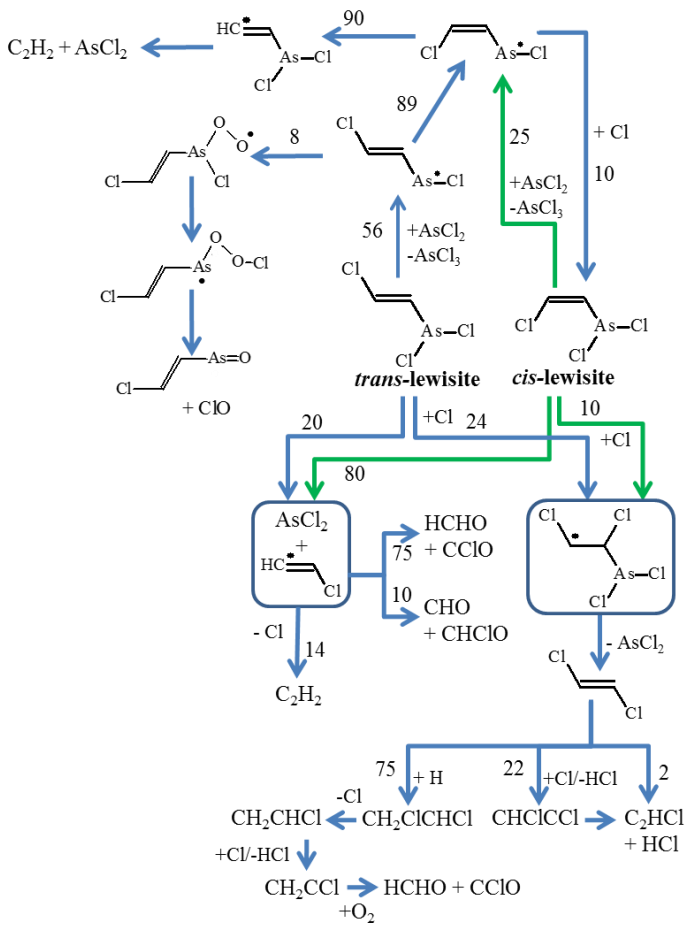

Figure 8: Flow analysis of decomposition of lewisite under combustion conditions in air. P = 1 bar, τ = 0.7 s, T = 773 K, Φ = 0.67, for a conversion of 30%.

Conclusion

A theoretical methodology of calculation properties of organoarsenics is proposed considering the large number of electrons in this atom, which allowed to investigate for the first time the most sensitive reactions of lewisite, a blister agent and a prototypal organoarsenic. An original comprehensive kinetic model of combustion of lewisite is proposed. Simulations in typical pyrolysis and combustion conditions shows the primary role of unimolecular decompositions due to the weak C—As bond, and Cl and $AsCl_2$ as chain carriers in the radical mechanism. The oxidation reactions become important at temperature higher than that of the lewisite decomposition and have little kinetic influence on lewisite destruction rate, but can however lead to specific arsenic oxides at low temperature. Simulations confirm the

experimental observation that lewisite yields $AsCl_3$ as the main arsenic product, but also arsenic oxides of potential high toxicity, such as AsOCl. Reaction of these small species, which will be present together during some solid combustion, such as coal or wastes, would disserve further investigations. The proposed methodology could also be applied to determine kinetics of contaminants such as pesticides or organoarsenic produced by microbial reduction of arsenic salts in municipal landfill (Li et al., 2011).

Acknowledgements

This work was supported by DGA Maîtrise NRBC. HPC resources were provide by the EXPLOR centre hosted by the University of Lorraine and by IDRIS under the allocation 2018-A0010807249 made by GENCI.

References

Ashmore, P.G., Owen, A.J., Robinson, P.J., 1982. Chlorine-catalysed pyrolysis of 1,2-dichloroethane. Part 2.—Unimolecular decomposition of the 1,2-dichloroethyl radical and its reverse reaction. J. Chem. Soc., Faraday Trans. 1 78, 677–693. https://doi.org/10.1039/F19827800677

Ayscough, P.B., Cocker, A.J., Dainton, F.S., Hirst, S., Weston, M., 1961. Excited chloroethyl radicals C2H2Cl5-x. Proc. Chem. Soc., London 244.

Baert, A., Danel, V., 2004. Armes chimiques. EMC - Toxicol.-Pathol. 1, 117–123. https://doi.org/10.1016/j.emctp.2004.03.001

Baronian, C., 1988. Chemical Stockpile Disposal Program: Final Programmatic Environmental Impact Statement. [U.S. Army Ordnance], Program Executive Officer--Program Manager for Chemical Demilitarization.

Buda, F., Bounaceur, R., Warth, V., Glaude, P.A., Fournet, R., Battin-Leclerc, F., 2005. Progress toward a unified detailed kinetic model for the autoignition of alkanes from C4 to C10 between 600 and 1200 K. Combust. Flame 142, 170–186.

Bunnett, J.F., Mikołajczyk, M., Division, N.A.T.O.S. and E.A., 1998. Arsenic and old mustard: chemical problems in the destruction of old arsenical and "mustard" munitions. Kluwer Academic Publishers.

Cheremisinoff, N.P., 1999. Handbook of Industrial Toxicology and Hazardous Materials. CRC Press.

Feller, D., Vasiliu, M., Grant, D.J., Dixon, D.A., 2011. Thermodynamic Properties of Arsenic Compounds and the Heat of Formation of the As Atom from High Level Electronic Structure Calculations. J. Phys. Chem. A 115, 14667–14676.

Frisch, M., Trucks, G., Schlegel, H., Scuseria, G., Robb, M., Cheeseman, J., Scalmani, G., Barone, V., Mennucci, B., Petersson, G., Nakatsuji, H., Caricato, M., Li, X., Hratchian, H., Izmaylov, A., Bloino, J., Zheng, G., Sonnenberg, J., Hada, M., Ehara, M., Toyota, K., Fukuda, R., Hasegawa, J., Ishida, M., Nakajima, T., Honda, Y., Kitao, O., Nakai, H., Vreven, T., Montgomery, J., Peralta, J., Ogliaro, F., Bearpark, M., Heyd, J., Brothers, E., Kudin, K., Staroverov, V., Kobayashi, R., Normand, J., Raghavachari, K., Rendell, A., Burant, J., Iyengar, S., Tomasi, J., Cossi, M., Rega, N., Millam, J., Klene, M., Knox, J., Cross, J., Bakken, V., Adamo, C., Jaramillo, J., Gomperts, R., Stratmann, R., Yazyev, O., Austin, A., Cammi, R., Pomelli, C., Ochterski, J., Martin, R., Morokuma, K., Zakrzewski, V., Voth, G., Salvador, P., Dannenberg, J., Dapprich, S., Daniels, A., Farkas, Foresman, J., Ortiz, J., Cioslowski, J., Fox, D., 2009. Gaussian 09, Revision D.01.

Goodall, A.M., Howlett, K.E., 1956. 520. The pyrolysis of chloroalkenes. Part III. The molecular mode of decomposition of the 1 : 2-dichloroethylenes. J. Chem. Soc. 2640–2646. https://doi.org/10.1039/JR9560002640

Gupta, R.C., 2015. Handbook of toxicology of chemical warfare agents. Academic Press.

Herron, J.T., 1988. Evaluated Chemical Kinetic Data for the Reactions of Atomic Oxygen O(3P) with Saturated Organic Compounds in the Gas Phase. J. Phys. Chem. Ref. Data 17, 967–1026. https://doi.org/10.1063/1.555810

Huybrechts, G., Narmon, M., Van Mele, B., 1996. The pyrolysis of CCl4 and C2Cl6 in the gas phase. Mechanistic modeling by thermodynamic and kinetic parameter estimation. Int. J. Chem. Kinet. 28, 27–36.

Kee, R.J., Rupley, F.M., Miller, J.A., 1993. CHEMKIN II. A Fortran Chemical Kinetics Package for the Analysis of Gas-Phase Chemical Kinetics. Sandia Laboratories Report, SAND 89-8009B.

Khalfa, A., Ferrari, M., Fournet, R., Sirjean, B., Verdier, L., Glaude, P.A., 2015. Quantum Chemical Study of the Thermochemical Properties of Organophosphorous Compounds. J. Phys. Chem. A 119, 10527–10539.

Leylegian, J.C., Zhu, D.L., Law, C.K., Wang, H., 1998. Experiments and Numerical Simulation on the Laminar Flame Speeds of Dichloromethane and Trichloromethane. Combust. Flame 114, 285–293.

Li, Y., Low, G.K.-C., Scott, J.A., Amal, R., 2011. Microbial transformation of arsenic species in municipal landfill leachate. J. Hazard. Mater. 188, 140–147. https://doi.org/10.1016/j.jhazmat.2011.01.093

Lizardo-Huerta, J.C., Sirjean, B., Bounaceur, R., Fournet, R., 2016. Intramolecular effects on the kinetics of unimolecular reactions of β-HOROO˙ and HOQ˙ OOH radicals. Phys. Chem. Chem. Phys. 18, 12231–12251.

Lizardo-Huerta, J.-C., Sirjean, B., Verdier, L., Fournet, R., Glaude, P.-A., 2018. Thermal Decomposition of Phosgene and Diphosgene. J. Phys. Chem. A 122, 249–257.

Louis, F., Gonzalez, C.A., Sawerysyn, J.-P., 2004. Direct Combined ab Initio/Transition State Theory Study of the Kinetics of the Abstraction Reactions of Halogenated Methanes with Hydrogen Atoms. J. Phys. Chem. A 108, 10586–10593.

Matheson, I., Tedder, J., Sidebottom, H., 1982. Photolysis of carbon tetrachloride in the presence of alkanes. Int. J. Chem. Kinet. 14, 1033–1045. https://doi.org/10.1002/kin.550140908

Nagymajtényi, L., Selypes, A., Berencsi, G., 1985. Chromosomal aberrations and fetotoxic effects of atmospheric arsenic exposure in mice. J. Appl. Toxicol. 5, 61–63. https://doi.org/10.1002/jat.2550050204

National Research Council (US) Subcommittee on Chronic Reference Doses for Selected Chemical Warfare Agents, 1999. Appendix F, Health Risk Assessment for Lewisite, Review of the U.S. Army's Health Risk Assessments For Oral Exposure to Six Chemical-Warfare Agents. National Academies Press (US).

Nowakowska, M., Herbinet, O., Dufour, A., Glaude, P.-A., 2014. Detailed kinetic study of anisole pyrolysis and oxidation to understand tar formation during biomass combustion and gasification. Combust. Flame 161, 1474–1488.

Pelucchi, M., Frassoldati, A., Faravelli, T., Ruscic, B., Glarborg, P., 2015. High-temperature chemistry of HCl and Cl2. Combust. Flame 162, 2693–2704.

Pohanish, R.P., 2008. Sittig's Handbook of Toxic and Hazardous Chemicals and Carcinogens, 5th Edition. William Andrew.

Pronicheva, L.D., Kuchkaev, B.I., Knyazev, B.A., 1992. Electron diffraction study of structure and internal rotation in molecule of β-chlorovinyldichloroarsine. J. Struct. Chem. 33, 673–677. https://doi.org/10.1007/BF00747073

Radke, B., Jewell, L., Piketh, S., Namieśnik, J., 2014. Arsenic-Based Warfare Agents: Production, Use, and Destruction. Crit. Rev. Environ. Sci. Technol. 44, 1525–1576.

Russell, J.J., Seetula, J.A., Gutman, D., Danis, F., Caralp, F., Lightfoot, P.D., Lesclaux, R., Melius, C.F., Senkan, S.M., 1990. Kinetics and thermochemistry of the equilibrium trichloromethyl radical + oxygen .dblarw. peroxotrichloromethane. J. Phys. Chem. 94, 3277–3283. https://doi.org/10.1021/j100371a012

Saeidian, H., Sahandi, M., 2015. Comprehensive DFT study on molecular structures of Lewisites in support of the Chemical Weapons Convention. J. Mol. Struct. 1100, 486–495. https://doi.org/10.1016/j.molstruc.2015.07.069

Sahu, C., Pakhira, S., Sen, K., Das, A.K., 2013. A Computational Study of Detoxification of Lewisite Warfare Agents by British Anti-lewisite: Catalytic Effects of Water and Ammonia on Reaction Mechanism and Kinetics. J. Phys. Chem. A 117, 3496–3506.

Sanderson, H., Fauser, P., Rahbek, M., Larsen, J.B., 2014. Review of environmental exposure concentrations of chemical warfare agent residues and associated the fish community risk following the construction and completion of the Nord Stream gas pipeline

between Russia and Germany. J. Hazard. Mater. 279, 518–526. https://doi.org/10.1016/j.jhazmat.2014.06.073
Sanderson, H., Fauser, P., Thomsen, M., Sørensen, P.B., 2007. PBT screening profile of chemical warfare agents (CWAs). J. Hazard. Mater. 148, 210–215. https://doi.org/10.1016/j.jhazmat.2007.02.027
Schuchardt, K.L., Didier, B.T., Elsethagen, T., Sun, L., Gurumoorthi, V., Chase, J., Li, J., Windus, T.L., 2007. Basis Set Exchange: A Community Database for Computational Sciences. J. Chem. Inf. Model. 47, 1045–1052.
Shea, D.A., Gottron, F., 2004. Small-Scale Terrorist Attacks Using Chemical and Biological Agents: An Assessment Framework and Preliminary Comparisons (CRS Report for Congress No. RL32391), CRS Report for Congress. Congressional Research Service, Washington, DC.
Smith, J.R., Logan, T.P., Szafraniec, L.L., Jakubowski, E.M., 1995. Spectroscopic Characterization of the Geminal Isomer of Lewisite. Anal. Lett. 28, 1541–1554.
Stone, H., See, D., Smiley, A., Ellingson, A., Schimmoeller, J., Oudejans, L., 2016. Surface decontamination for blister agents Lewisite, sulfur mustard and agent yellow, a Lewisite and sulfur mustard mixture. J. Hazard. Mater. 314, 59–66. https://doi.org/10.1016/j.jhazmat.2016.04.020
Stull, D.R., 1947. Vapor Pressure of Pure Substances. Organic and Inorganic Compounds. Ind. Eng. Chem. 39, 517–540. https://doi.org/10.1021/ie50448a022
Tsang, W., Hampson, R.F., 1986. Chemical Kinetic Data Base for Combustion Chemistry. Part I. Methane and Related Compounds. J. Phys. Chem. Ref. Data 15, 1087–1279. https://doi.org/10.1063/1.555759
Urban, J.J., von Tersch, R.L., 1999. Conformational analysis of the isomers of lewisite†. J. Phys. Org. Chem. 12, 95–102.
Weigend, F., Ahlrichs, R., 2005. Balanced basis sets of split valence, triple zeta valence and quadruple zeta valence quality for H to Rn: Design and assessment of accuracy. Phys. Chem. Chem. Phys. 7, 3297–3305.
Zhang, W., Du, B., Feng, C., 2007. An ab initio dynamics study on the reaction of O(3P) with CH3CHCH2 (1A′). J. Mol. Struct. THEOCHEM 806, 121–129. https://doi.org/10.1016/j.theochem.2006.11.014
Zhang, W., Guo, X., Zhang, Y., Wang, F., Shi, H., Zhang, J., Wang, R., Tang, S., Wang, H., Sun, H., 2014. The mechanistic study of the hydroxyl radical reaction with trans-2-chlorovinyldichloroarsine. J. Mol. Model. 20, 2335.
Zhang, Z., Liu, J., Shen, F., Dong, Y., 2020. Temporal influence of reaction atmosphere and chlorine on arsenic release in combustion, gasification and pyrolysis of sawdust. J. Hazard. Mater. 382, 121047. https://doi.org/10.1016/j.jhazmat.2019.121047

Supplemental material

“Lewisite_mech”: Detailed kinetic mechanism.